https://doi.org/10.31925/farmacia.2025.6.15 **ORIGINAL ARTICLE**

SYNTHESIS, CHARACTERISATION AND A PRELIMINARY *IN VITRO* EVALUATION OF A MAGNETIC NANOFORMULATION ON KIDNEY VERO CELL LINE

MIHAI CRISTIAN NEAGU [1,2], EUGEN SORIN BOIA [1], PAULA ALEXANDRA ANDRICĂ [2]*, ANDREEA MARIA CRISTEA [3,4], DANIELA SASCO [3], FLAVIUS BOB [1,5,6], ANDREEA SMEU [3,4], ALINA ANTON [3,4], ELENA-ALINA MOACĂ [3,4]

[1]*Faculty of Medicine, "Victor Babeş" University of Medicine and Pharmacy Timişoara, 2nd Eftimie Murgu Square, 300041 Timişoara, Romania*
[2]*Doctoral School of Medicine, "Victor Babeş" University of Medicine and Pharmacy Timişoara, 2nd Eftimie Murgu Square, 300041 Timişoara, Romania*
[3]*Faculty of Pharmacy, "Victor Babeş" University of Medicine and Pharmacy Timişoara, 2nd Eftimie Murgu Square, 300041 Timişoara, Romania*
[4]*Research Centre for Pharmaco-Toxicological Evaluations, "Victor Babeş" University of Medicine and Pharmacy Timişoara, 2nd Eftimie Murgu Square, 300041 Timişoara, Romania*
[5]*Centre for Molecular Research in Nephrology and Vascular Disease, "Victor Babeş" University of Medicine and Pharmacy, 2nd Eftimie Murgu Square, 300041 Timişoara, Romania*
[6]*County Emergency Hospital, 156 L. Rebreanu Street, 300723 Timişoara, Romania*

**corresponding author: andricapaula@gmail.com*

Manuscript received: October 2025

Abstract

The present study aimed to synthesise, characterise and evaluate *in vitro* a magnetic colloidal suspension (MCS) based on magnetic iron oxide nanoparticles (MIONPs) obtained by the combustion method and double-coated with vegetable oleic acid (OA), dispersed in aqueous media. Physical-chemical investigations showed that the synthesised sample (MCS_OA) has a hydrodynamic diameter (Dh) of 43.13 nm, a polydispersity index (PDI) of 0.524, a saturation magnetisation (Ms) of 1.06 Gs and an average particle size of 18.1 ± 2.1 nm with a narrow distribution of nanoparticle sizes determined by transmission electron microscopy (TEM). Preliminary *in vitro* analyses were performed after 24 hours of exposure on the Vero kidney cells. The results indicated that MCS_OA induces a dose-dependent decrease in cell viability, especially at a 2 µg/mL concentration, which was also confirmed by morphological changes in cells and by nuclear and mitochondrial dysmorphologies. Collectively, MCS_OA warrants additional research into its therapeutic potential, although further investigation is needed to ensure safety and efficacy in clinical applications.

Rezumat

Acest studiu a avut ca scop sintetizarea, caracterizarea și evaluarea *in vitro* a unei suspensii coloidale magnetice (MCS) pe bază de nanoparticule magnetice de oxid de fier (MIONP) obținute prin metoda combustiei și acoperite dublu cu acid oleic vegetal (OA), dispersate în mediu apos. Investigațiile fizico-chimice au arătat că proba sintetizată (MCS_OA) are un diametru hidrodinamic (Dh) de 43,13 nm, un indice de polidispersie (PDI) de 0,524, o magnetizare de saturație (Ms) de 1,06 Gs și o dimensiune medie a particulelor de 18,1 ± 2,1 nm, cu o distribuție îngustă a dimensiunilor nanoparticulelor determinată prin microscopie electronică de transmisie (TEM). Analizele preliminare *in vitro* au fost efectuate după 24 de ore de expunere pe celulele renale Vero. Rezultatele au indicat că MCS_OA induce o scădere dependentă de doză a viabilității celulare, în special începând cu o concentrație de 2 µg/mL, ceea ce a fost confirmat și de aspectele morfologice ale celulelor, precum și de dismorfologiile nucleare și mitocondriale care au survenit. În ansamblu, MCS_OA justifică cercetări suplimentare privind potențialul său terapeutic, deși sunt necesare investigații suplimentare pentru a asigura siguranța și eficacitatea în aplicațiile clinice.

Keywords: magnetic colloidal suspension, combustion synthesis, cytotoxicity, biosafety, kidney cells

Introduction

Currently, there is significant interest in synthesising nanomaterials with controllable properties that can selectively interact with human cells or tissues, transport active molecules, or provide accurate diagnostic information [13, 80, 86]. This interest is primarily driven by the ability to adjust the physicochemical characteristics of nanomaterials (such as size, shape, surface chemistry and responsiveness to stimuli) to enable targeted biodistribution in the human body and effective delivery of potential therapeutic agents from their surfaces [10, 13, 79, 80, 86]. The progress made to date in integrating the therapeutic and diagnostic functions of these nanomaterials is considered a path toward more precise and rapid interventions, particularly

in oncology, but also in other complex diseases [10, 44, 84, 86].

Magnetic iron oxide nanoparticles (MIONPs) represent one of the most studied categories of nanomaterials. MIONPs have become well-known nanomaterials not only for their tailored physico-chemical properties but also for their abilities of increased biocompatibility and reduced toxicity [29, 40, 49, 50, 66, 72, 90]. Magnetite (Fe_3O_4) and its oxidised form, maghemite (γ-Fe_2O_3), are two compounds acknowledged as outstanding candidates for biomedical applications [54]. It has been found that applications with magnetic nanoparticles composed of nickel, cobalt and iron have the potential to bring significant value to the advancement and development of innovative therapies based on these principles, including in oncology [23]. An important role is also played by evaluating the biosafety of compounds before their implementation as potential therapeutic agents. Moreover, the functionalised compound on the MIONPs surface or the surfactant (the protective layer) needs to be non-toxic and biocompatible to ensure high colloidal stability across different carriers, prevent MIONP aggregation, sedimentation and, ultimately, biodegradation [29, 40, 72].

One of the aggressive cancers that urgently needs attention in terms of finding new treatment alternatives is kidney cancer. Kidney cancer (KC) is a disease with an incidence of approximately 400,000 cases annually and a death rate of 175,000 *per* year [15]. Renal cell carcinoma (RCC) develops from the renal parenchyma. It ranks 13th worldwide among the most common types of cancer, accounting for 2.4% of all cancer cases, occurring twice as often in men as in women [70]. Today, treatments available for patients with this type of cancer vary, but generally include surgery, radiation therapy, targeted therapy (*e.g.*, axitinib, bevacizumab, cabozantinib, everolimus, sorafenib) and immunotherapy (*e.g.*, avelumab, interferon, nivolumab). However, these treatments often lead to toxic side effects; therefore, new drugs are being tested in various clinical trials to find alternatives [89]. The anticancer drugs have numerous side effects that exacerbate the suffering of cancer patients [3], and the other types of therapies listed also induce complications [14, 87, 77]. Preclinical *in vitro* studies on the use of MIONPs for labelling, imaging, or targeting renal cells are limited, with most focusing on renal cancer or labelling strategies that may apply to healthy renal epithelium [12, 17-19, 37, 46]. To the best of our knowledge, there are no clinical studies reporting the use of MIONPs in healthy renal epithelial cells or in renal cancer. The current clinical context focuses on broader uses of superparamagnetic iron oxide nanoparticles (SPIONs), such as the treatment of anaemia associated with chronic kidney disease [51] or concepts of hyperthermia and imaging, rather than targeting renal cell carcinoma [18, 30, 88], with no evidence of impact on healthy renal epithelium or applicability in renal cancer. This highlights gaps identified in the literature regarding preclinical and clinical research on the use of MIONPs on renal function. Therefore, *in vitro* toxicological and biosafety assessments specific to healthy renal cell lines prior to any assessment focused on renal cell carcinoma are essential [39].

The primary objective of this research was to manufacture and characterise a magnetic colloidal suspension (MCS) based on MIONP coated with a double layer of vegetable oleic acid (OA) and dispersed in distilled H_2O (MCS_OA). The secondary objective is to assess the toxicological profile of the MCS_OA in Vero cells, a continuous cell line derived from renal epithelial cells, frequently used for toxicological screening due to its availability for future studies on its anticancer potential, including in the case of renal cancer.

Materials and Methods

Reagents used in the synthesis process

For the synthesis of magnetic iron oxide nanoparticles (MIONPs) through the combustion method, the ($Fe(NO_3)_3 \times 9\ H_2O$, from Carl Roth, Germany), and citric acid monohydrate ($C_6H_8O_7 \times H_2O$, from Silal Trading, Romania) were employed as the starting raw materials. For the synthesis of magnetic colloidal suspension (MCS), the oleic acid (OA) $C_{18}H_{34}O_2$ (from Merck, 65 - 88%) was used as surfactant, alongside ethanol (70%, v/v), used as magnetic nanoparticles moisturizing aqueous solution, NH_4OH (25%), as pH regulation solution and distilled water, used as magnetic nanoparticles dispersion carrier media.

Synthesis of MIONPs through the combustion method and the preparation of MCS

The oxidising agent and the fuel were dissolved in 50 mL of distilled water and subjected to combustion at 400°C in a heating mantle in the absence of air, as previously described in detail in reference [33]. The recipe was designed to obtain 0.03 mol of MIONPs using a stoichiometric metal nitrate (oxidising agent)/ fuel (reducing agent) molar ratios, according to the following reaction:

$$54\ Fe(NO_3)_3 + 46\ C_6H_8O_7 \rightarrow 18\ Fe_3O_4 + 276\ CO_2 + 184\ H_2O + 81\ N_2.$$

The MIONPs obtained were washed several times with distilled water and dried in an oven at 80°C. After drying, the MIONPs were coated with a double layer of OA, as described in the modified protocol by Bica *et al*. [5]. Briefly, the MIONPs obtained *via* combustion were left to soak for 1 day in an aqueous solution of ethanol (70%, v/v) and distilled water at a 1:20 volumetric ratio. The suspension was sonicated for 2 h at 50% amplitude, then subjected to thermomagnetic stirring using a magnetic bar. When the temperature of the mixture reached 80 - 82°C, the first layer of OA was added dropwise under vigorous stirring (500 rpm). The MIONPs were single-coated with OA and washed several times with warm distilled

water (60 - 70°C) to remove soluble impurities and free oleic acid. The MIONPs, single-coated with OA, were redispersed in distilled water and subjected to the thermomagnetic stirring process again. By using a 25% NH_4OH solution, a basic pH in the aqueous suspension (pH = 10.27) was ensured, and when the aqueous suspension reached 80 - 82°C, the MIONPs were coated with the OA second layer. Thus, the MIONPs double-coated with OA were decanted using a magnet and dispersed in distilled water by sonication (50% amplitude) for 1 h. Finally, a magnetic colloidal suspension of oleic acid double-layer-coated iron oxide magnetic nanoparticles was obtained, which was further characterised and analysed herein after as MCS_OA (Figure 1).

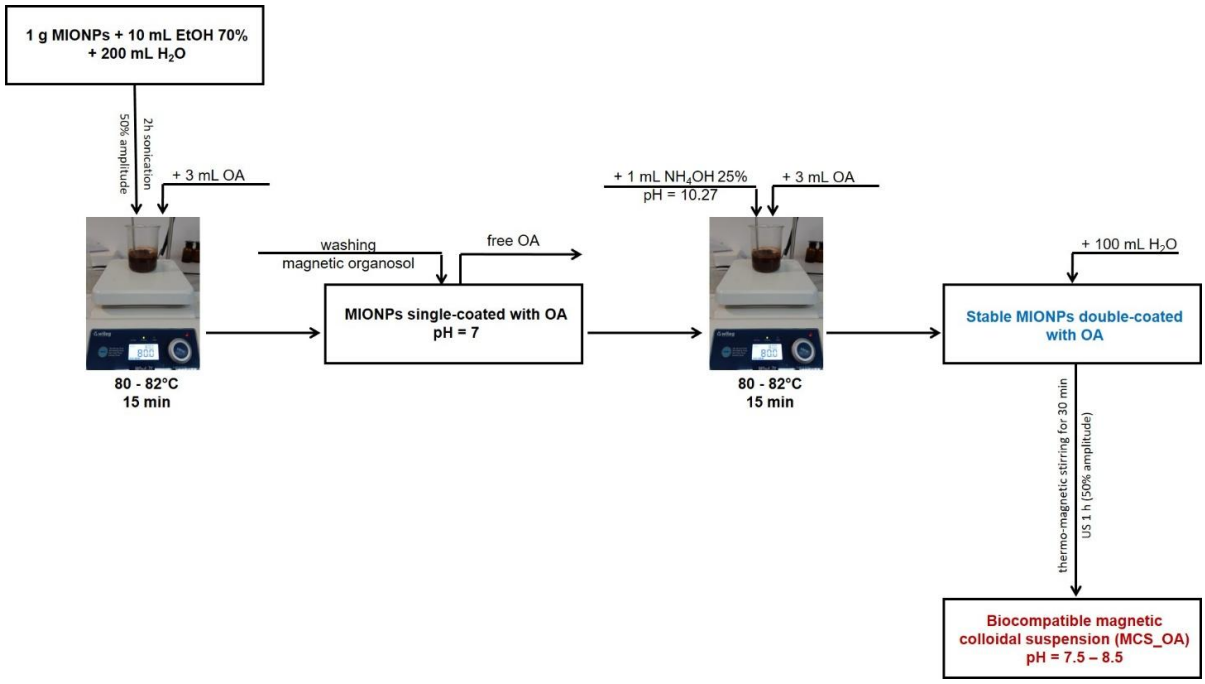

Figure 1.
Schematic protocol of stable magnetic colloidal suspension preparation

Characterisation of the MIONPs and MCS_OA

After synthesising the MCS_OA, the mass of iron oxide in the sample was calculated. For this, the density of the MCS_OA sample was first measured using a portable Density Meter (DMA 35) from Anton Parr at 25°C. Based on this density, the volume fraction of the MCS_OA sample was calculated, using the following equation:

$$\varphi = \frac{\rho_{MCS\_OA} - \rho_{H2O}}{5.2 - \rho_{H2O}}, \qquad \text{Eq. (1)}$$

where, φ = volume fraction; ρ_{MCS_OA} = the density of the sample; ρ_{H2O} = the density of the carrier medium (which in our case is the distilled water – 0.9465 g/cm^3); 5.2 = the theoretical density of Fe_3O_4.

The MIONPs were characterised in terms of XRD phase composition (Rigaku Ultima IV, Tokyo, Japan), specific surface area (Micromeritics ASAP 2020, Norcross, USA), and magnetic properties using a VSM 880 ADE/DMS magnetometer from Massachusetts, USA.

The MCS_OA sample was characterised for hydrodynamic diameter by dynamic light scattering (DLS) using a ZetaSizer NanoZS from Malvern Instruments (Worcestershire, UK). Using scanning (SEM) and transmission electron microscopy (TEM), we determined changes in the morphology and ultrastructure of aggregates with a FEI Tecnai 12 Biotwin electron microscope from Oregon, USA. For the SEM analysis, the microscope used was an FEI Quanta 250 from Eindhoven, The Netherlands, equipped with an ETD (Everhart-Thornley detector for secondary electrons). The elemental analysis of the chemical compounds, as well as their weight relative percentage (Wt%) in the MCS_OA sample, was investigated using EDX (energy-dispersive X-ray spectroscopy) on an EDAX Apollo X detector from Ametek, Mahwah, USA.

Reagents and equipment used for in vitro experiments

For the *in vitro* experiments, the phosphate-buffered saline (PBS) and the MTT (3-(4,5-dimethylthiazol-2-yl)-2,5-diphenyltetrazolium bromide) viability kit were obtained from Sigma-Aldrich, Merck KGaA (Darmstadt, Germany). The Eagle's Minimum Essential Medium (EMEM), foetal bovine serum, penicillin/streptomycin mixture and trypsin-EDTA solution were purchased from American Type Culture Collection (ATCC), Manassas, VA, USA. The dimethyl sulfoxide, DMSO, (solvent) was procured *via* PAN-Biotech GmbH, Aidenbach, Germany. Hoechst 33342 and MitoTracker™ Red CMXRos were acquired from

Thermo Fisher Scientific (Waltham, MA, USA). The equipment used, Cytation 5 (plate reader) and Lionheart FX (automated microscope), was obtained from BioTek Instruments Inc. (Winooski, VT, USA).

Cell culture protocol

In this work, *in vitro* experiments were conducted on the Vero normal kidney cell line (CCL-81™) from the American Type Culture Collection (ATCC), Manassas, VA, USA. The cell line was cultured in the specific growth medium EMEM supplemented with 10% FBS and 1% antibiotic mixture. During the experiments, Vero cells were maintained in a humidified incubator at 37°C and 5% CO_2.

Cellular viability evaluation

For the cell viability test, kidney Vero cells were grown in 96-well plates until the desired confluence and treated with the sample of interest (MCS_OA) at concentrations of 1, 2, 3, 4 and 5 µg/mL for 24 hours. After treatment, the culture medium was replaced with fresh medium, and 100 µL of MTT kit 1 was added using a multichannel pipette (incubated for 3 hours). Subsequently, 10 µL of MTT solubilising solution was applied for 30 minutes, during which time the plates were incubated at room temperature. Finally, the absorbance was read at 570 and 630 nm using the Cytation 5 instrument [56].

Bright-field morphological examination

Morphological analysis of Vero cells was performed 24 hours after treatment with MCS_OA at 1, 2, 3, 4 and 5 µg/mL using the Lionheart FX automated microscope, following the instructions of Romănu *et al*. [67].

Mitochondrial immunofluorescence staining via Mito-Tracker™ Red CMXRos and Hoechst 33342 nuclear assessment

The nuclear and mitochondrial aspects of the cells were evaluated using the Hoechst 33342 nuclear staining and MitoTracker™ Red CMXRos immunofluorescence staining.

To analyse mitochondrial morphology, Vero cells were cultured in 12-well plates and allowed to adhere until optimal confluence was reached. Subsequently, treatment was applied for 24 hours at concentrations of 1, 3 and 5 µg/mL. The MitoTracker dye was initially dissolved in DMSO at a stock concentration of 1 mM and then diluted in the specific culture medium for each cell line to a final concentration of 300 nM. Following a 30-minute incubation with the staining solution under standard culture conditions, the cells were washed with culture medium to remove excess dye. Then, after staining with MitoTracker, the cells were fixed with 4% paraformaldehyde for 10 minutes at room temperature to preserve the cell structures, followed by a thorough wash with PBS.

To verify the nuclear changes induced in the cells under investigation by the sample of interest (MCS_OA), cells were stained with Hoechst 33342. After fixation, Hoechst 33342 solution (diluted 1:2000 in PBS) was added to each well and incubated for 5 - 10 minutes in the dark. The staining solution was then removed, and the wells were washed three times with PBS.

Representative fluorescent images were acquired by using the Lionheart FX automated microscope at 20× magnification. Image analysis was performed by using Gen5™ Microplate Data Collection and Analysis software (version 3.14; BioTek Instruments Inc., Winooski, VT, USA).

Statistical analysis

The obtained results were analysed using GraphPad Prism software (GraphPad® Software, San Diego, CA, USA, www.graphpad.com), Version 9.3.1. The differences between the cells treated with MCS_OA and control were determined using One-way ANOVA and Dunnett's multiple comparison tests. All statistically significant results were marked with "*", as follows: *$p < 0.05$; **$p < 0.01$; ***$p < 0.001$; ****$p < 0.0001$.

Results and Discussion

Nowadays, nanotechnology is increasingly used in medical practice due to its ability to provide nano-scale solutions to various complex medical problems, such as early diagnosis, targeted therapies and real-time monitoring of biological processes. Among the factors that have led to the increased use of this field in medicine are advanced nanoscale material manufacturing, the ability to control physicochemical properties during production, improved biocompatibility, enhanced surface functionalisation capacity and easy integration with modern imaging techniques or therapeutic systems [9, 22, 53, 69, 75, 91, 93]. Magnetite (Fe_3O_4) and maghemite (γ-Fe_2O_3), due to their distinct magnetic properties, particularly the superparamagnetic behaviour exhibited at sizes below ~ 20 nm, are integrated into numerous biomedical applications. These nanomaterials are widely used as carriers for targeted drug delivery, contrast agents in magnetic resonance imaging (MRI), magnetic separation and cell selection, magnetofection, tissue repair and magnetic hyperthermia, a cancer treatment in which nanoparticles, subjected to an alternating magnetic field, generate enough heat to induce selective death of tumour cells [25, 47, 49, 50, 55, 63, 66, 68, 71, 92].

In order to obtain magnetic iron oxide nanoparticles with suitable properties for biomedical applications, the synthesis method is particularly important; it must be simple, accessible and environmentally friendly. Various synthesis methods have been employed to manufacture MIONPs with tailored properties, including coprecipitation [27, 81, 90], hydrothermal/solvothermal [21, 95], microemulsion [20, 29, 60, 90], sonochemical [38, 58, 81, 90], thermal decomposition [32, 42, 90] and electrochemical [41, 90]. However, these methods have significant limitations in the preparation of magnetic nanomaterials [38, 42, 90], which justifies the need for new, simple and efficient approaches.

The combustion method is a promising alternative to conventional synthesis methods, as it is simple, energy-efficient, fast, versatile, environmentally friendly and low-cost. This method is based on an exothermic reaction between an oxidising agent (metal nitrate) and a reducing agent (fuel). It is used to obtain metal oxides [4, 34, 35, 62, 76] and, increasingly frequently, for the manufacture of MIONPs [31, 33, 59, 74, 85], allowing their properties to be adjusted by varying synthesis conditions.

Biocompatible surfactants (such as polyethylene glycol, fatty acids, Tween 80, dextran, starch, chitosan, *etc.*) are used to functionalise the surface of nanoparticles. Of these, vegetable oleic acid is the most widely used, forming a dense, protective layer that ensures uniform, monodisperse nanoparticles [94].

This study is focused on the synthesis and characterisation of MIONPs using the combustion method, followed by the preparation of a biocompatible magnetic colloidal suspension based on these nanoparticles coated with a double layer of vegetable oleic acid (sample MCS_OA). The MIONPs employed for the obtaining of the bio-compatible MCS_OA, as well as their physicochemical characterisation, were previously published by our research group in reference [33]. In Table I, the physicochemical properties of MIONPs used to obtain the MCS_OA are briefly presented.

Table I

The physicochemical properties of MIONPs used to obtain the MCS_OA sample [33]

Fuel	Reaction condition	XRD phase composition	D_{XRD} [nm]	S_{BET} [m^2/g]	D_{BET} [nm]	Ms [emu/g]	Mr [emu/g]	Hc [kA/m]
citric acid	absence of air	Fe_3O_4	18	56	21	57.7	4.5	5.2

One can observe that the saturation magnetisation of the MIONPs obtained through the combustion method (Ms = 57.7 emu/g) was relatively higher, considering that the saturation magnetisation of bulk Fe_3O_4 at room temperature ranges between 80 and 90 emu/g [26, 28], even higher (90 - 100 emu/g) depending on the study's report measurement [65]. Moreover, the remanent magnetisation and the coercivity of the magnetic nanoparticles were close to the superpara-magnetic behaviour.

A high specific surface area (S_{BET}) indicates small nanoparticles. Our results regarding the specific surface area are well correlated with the BET diameter, indicating that the synthesised MIONPs obtained by the combustion method have a narrow size distribution, with nanoparticles under 50 nm. The size of nanoparticles is suitable for intravenous administration, in addition to other bio-medical applications that require larger nanoparticles (drug delivery vectors, MRI contrast agents, hyper-thermia therapy) [7, 24].

To obtain the magnetic colloidal suspension (MCS) and avoid magnetic nanoparticle agglomeration, characteristic of particles with a large surface-to-volume ratio, a vegetable oleic acid coating agent was used to isolate the nanoparticles, leading to monodisperse nanoparticles [43, 52]. A double layer of OA was used to disperse the MIONPs in aqueous solution; a single layer of OA makes the MIONPs dispersible only in organic solvents due to the hydrophobic tail of OA, which limits their biomedical applications [64]. By applying Eq. (1), the volume fraction of the sample was calculated to determine the mass of iron oxide contained in the MCS_OA sample. Knowing the density of the sample (ρ = 0.9956 g/cm^3), the density of the carrier medium (distilled water; ρ = 0.9465 g/cm^3) and the theoretical density of Fe_3O_4 (ρ = 5.2 g/cm^3), we were able to calculate the volume fraction of the sample (φ = 0.00998). Therefore, the mass of iron oxide calculated/mL of magnetic colloidal suspension, taking into account the theoretical density of Fe_3O_4, was 0.0520 g.

The MCS_OA double-coated was further characterised in terms of saturation magnetisation, DLS and TEM analyses. The saturation magnetisation measured with the VSM 880 ADE/DMS magnetometer showed a value of 1.06 Gs for magnetic colloidal suspension (MCS_OA).

The particle size distribution was assessed using dynamic light scattering (DLS). The results recorded are presented in Figure 2, by the intensity of the particles as well as by the volume of particles. One can observe that the average hydrodynamic diameter (Dh) of the MCS_OA sample was 43.13 nm. A confirmation of the double-layer oleic acid on the surface of the MIONPs is the difference between the hydrodynamic diameter (43.13 nm) of the MCS_OA sample and the diameter determined from the XRD analysis (D_{XRD} = 18 nm). Ultimately, these diameters cannot be compared because the first measures the hydrodynamic diameter of the colloid, while the second measures the average size of the crystallites.

The distribution by intensity shows that the sample was primarily composed of a single family of nanoparticles: 96.1% had a Dh of 82.96 nm, and only 3.9% had a Dh of 3075 nm. On the other hand, the distribution by volume shows two clear families of nanoparticles: 30.0% were 3.83 nm and 69.4% were 10.71 nm. A very small percentage of 0.5% were found to have 4073 nm.

The polydispersity index (PDI) was 0.524, indicating that the large nanoparticles in the MCS_OA sample are prone to flocculation and sedimentation.

In the DLS analysis, the PDI index is a dimensionless parameter that quantifies the breadth of the particle-size distribution. This index describes the degree of monodispersity (narrow) or polydispersity (wide) of a sample, being defined for a single population of

nanoparticles [1]. In our case, a magnetic colloidal suspension, this index denotes the uniformity of the magnetic nanoparticles, which, in turn, affects the collective magnetic behaviour of the sample, the heating, transport and stability of the nanoparticles in suspension [1]. Therefore, in DLS analysis, low PDI values correspond to narrow, almost monodisperse distributions. In contrast, high PDI values indicate broader size distributions, which may reflect polydispersity or aggregation of the magnetic nanoparticles. Furthermore, various literature reports PDI values around 0.57, indicating broad distributions typical of magnetic nanoparticles dispersed in complex media, where aggregation or coating heterogeneity can broaden the size distribution [45, 61]. Our result is consistent with these studies, highlighting that even magnetic colloidal suspensions used in biomedical contexts can exhibit moderately high PDI values when aggregation is present or when a wide range of particle sizes is stabilised in suspension. [45, 61].

Based on our results, one can affirm that the prepared MCS_OA sample is suitable for *in vitro* applications, as the hydrodynamic diameter falls within the range established for the biomedical domain (< 100 nm) [52, 78].

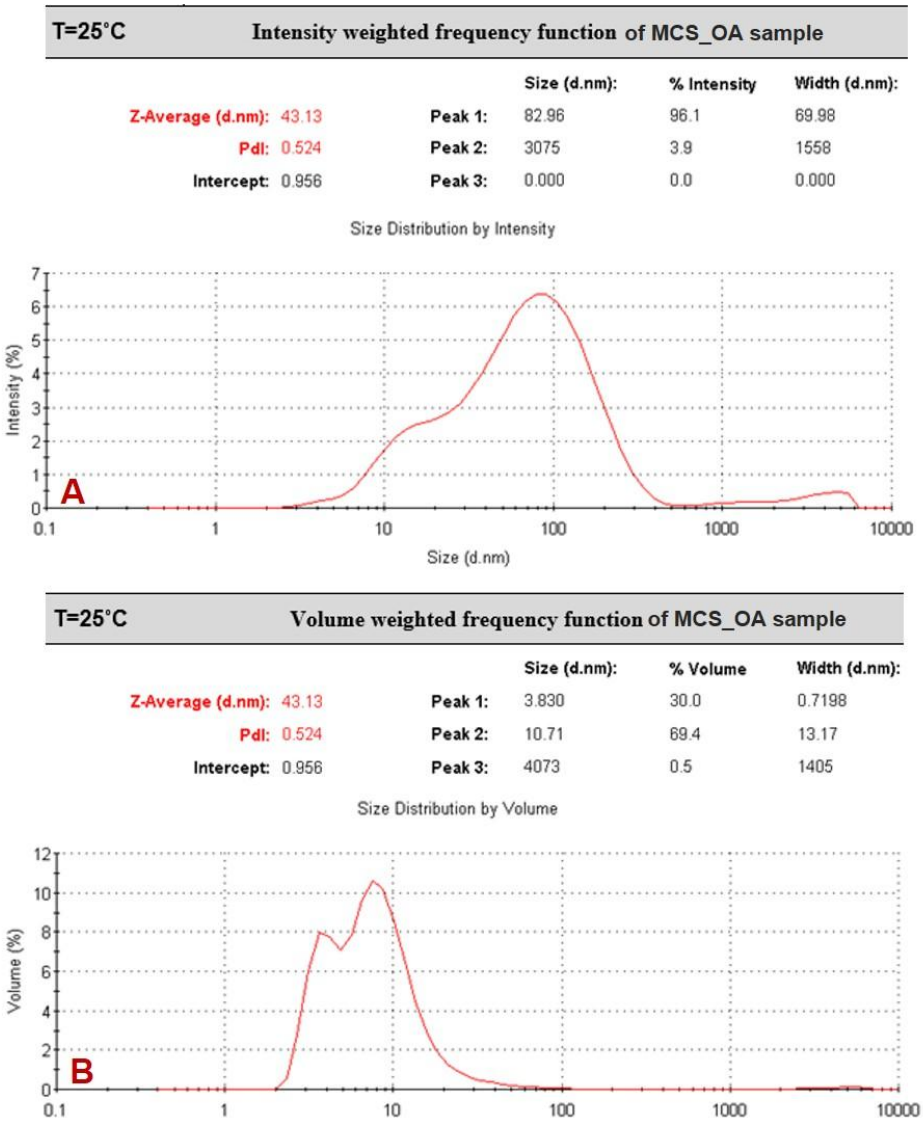

Figure 2.
The size distribution of the particles contained in the MCS_OA sample – A) by intensity and B) by volume

In Figure 3, TEM and SEM micrographs of the MCS_OA are shown, depicting the morphology and ultrastructure of the magnetic colloidal suspensions. Regarding the morphology of the colloidal nanosystem (Figure 3B), one can observe that the nanoparticles have quasi-spherical shapes, are arranged quasi-uniformly, are slightly agglomerated, exhibit a narrow size distribution, and have a mean particle size of 18.1 ± 2.1 nm. The elemental composition of the magnetic colloidal nanosystem, as determined by EDX analysis, showed that C (Wt = 78.3%), O (Wt = 7.9%) and Fe (Wt = 13.8%) are the only elements present in

the sample. The EDS mapping (used to estimate the relative abundance of the chemical elements present in the magnetic colloidal nanosystem) (Figure 3C) is in agreement with the EDX profile of the MCS_OA sample. The mapping analysis was performed to determine whether the elements present in the sample are dispersed and homogeneous, and it confirmed the presence of C, O and Fe atoms. Our results confirmed the synthesis of narrow-sized particles, in accordance with literature data [8, 52, 78, 83].

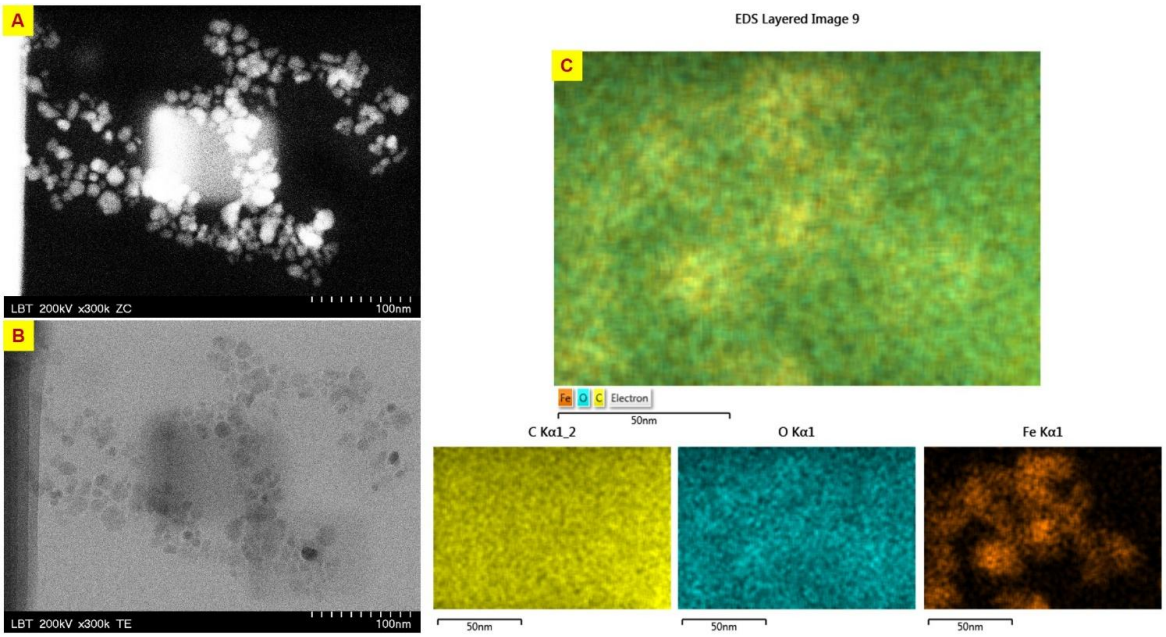

Figure 3.
The MCS_OA sample: A) SEM image; B) TEM image; C) mapping of the magnetic colloidal suspension

Nowadays, because of the limitations, treatment resistance, non-response and side effects of conventional treatments for kidney cancer, there is a need for new therapeutic options [14, 77]. Regarding the surgical procedures, the risks and complications depend on age and comorbidities [87]. The toxicity of new targeted drugs can reduce their effectiveness in advanced renal cancer if it is not detected promptly and treated appropriately. As a specific example, sorafenib, temsirolimus and bevacizumab cause toxicity by targeting healthy tissues, leading to delays or interruptions in drug treatment [77]. Although many of the treatments developed to date have achieved significant progress, challenges remain, particularly regarding treatment resistance (sunitinib frequently induces drug resistance within approximately six months of treatment) and the emergence of non-response to treatment, which complicates management. Other challenges include the adverse effects of targeted therapies and immune inhibitors, which cause liver toxicity, gastrointestinal problems and even bone marrow suppression [14]. Also, before implementing a new treatment, a bio-safety assessment is mandatory to assess how healthy tissues respond; one of the limitations of conventional cancer therapies is their toxic effects on healthy organs. In this sense, after the physical-chemical characterization, the second part of the study consisted of the preliminary *in vitro* evaluation of the magnetic colloidal suspension based on magnetic iron oxide nanoparticles (MIONPs), more exactly magnetite (Fe_3O_4), coated with a double layer of vegetable oleic acid (OA) and dispersed in H_2O (MCS_OA) on a 2D Vero cell model. In this context, the following were evaluated: cell viability using the MTT method, morphological analysis, cell nuclei and mitochondrial appearance of both cell types after a 24-hour treatment with the MCS_OA sample at concentrations ranging from 1 to 5 µg/mL. Vero cells are normal renal epithelial cells derived from the *Cercopithecus aethiops* organism [2].

The first part of the toxicological profile evaluation of MCS_OA consisted of an MTT assay to assess cell viability after 24 hours of treatment. The MTT method is often used as a colourimetric assay to determine cell viability, proliferation and cytotoxicity. The mechanistic principle of MTT is based on the ability of living cells to convert the yellow MTT tetrazolium salt into purple formazan crystals; thus, this colour change from yellow to purple provides a visual signal for cell viability [57].

Treatment of Vero cells (Figure 4) with the sample of interest, MCS_OA, resulted in a dose-dependent decrease in viability. Compared to the control, the percentages of viable cells were 76.08% at 1 µg/mL, 75.37% at 2 µg/mL, 29.17% at 3 µg/mL and approximately 22% at both 4 µg/mL and 5 µg/mL.

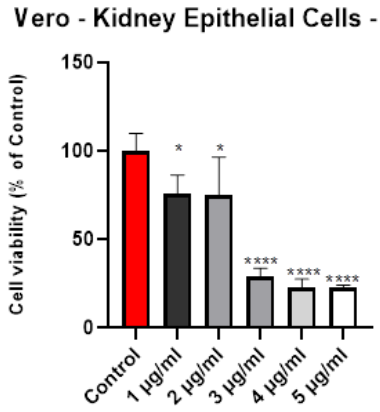

Figure 4.

Representation of cell viability percentages 24 h after treatment of Vero cells with various concentrations (1 - 5 µg/mL) of MCS_OA sample

The results are presented as percentages (%) normalised to control. All data are expressed as mean values ± SD from three independent experiments done in triplicate. The One-way ANOVA test was conducted to analyse differences between the control and treated groups, followed by Dunnett's multiple-comparison post hoc test. "*" marks statistical significance (* $p < 0.05$ and **** $p \leq 0.0001$)

Cell viability is the proportion of living, healthy cells in a given population. Moreover, for the pharmaceutical industry, it also plays a crucial role in selecting potential therapeutic candidates and determining their safe dosages. Overall, this type of assessment aims to understand cellular processes and the biological effects of compounds [48]. Fe_3O_4 nanoparticles have already been found to induce modifications in human A375 cells and murine B164A5 melanoma cells [54]. Furthermore, the utility of magnetic nanoparticles in the biomedical domain has attracted growing interest due to their fundamental biological, chemical and magnetic properties, which include biocompatibility, chemical stability and high magnetic susceptibility [73]. In comparison with the current work, another study by Moacă *et al*. involving a magnetic colloidal suspension (MCS) based on citric acid-coated magnetic iron oxide nanoparticles reported that the MTT cell viability assay showed that MDA-MB-231 and MCF-7 cells were not significantly affected by the 24-hour treatment [54]. Coricovac *et al*. investigated biocompatible colloidal suspensions obtained by coating magnetic iron oxide nanoparticles resulting from the combustion synthesis of the solution with a double layer of oleic acid. They assessed their effects on normal keratinocyte cells (HaCat) for 24 hours at doses of 5, 10 and 25 µg/mL. Their *in vitro* data proved that these suspensions do not induce cytotoxicity in keratinocytes, according to the Alamar Blue cell viability assay, and, moreover, the acute dermal toxicity test revealed that topical applications of colloidal suspensions on female and male SKH-1 hairless mice did not induce skin alterations [16].

The following step in evaluating the cytotoxicity of MCS_OA was at the morphological level. In healthy Vero cells (Figure 5), treatment with 1 µg/mL MCS_OA produced a slight decrease in cell confluence, which progressively continued with treatment at a concentration of 2 µg/mL. Starting with treatment at a dose of 3 µg/mL up to 5 µg/mL, the cells gradually decrease in confluence, exhibiting signs of cellular stress, as marked by dysmorphologies such as cell rounding and cell shrinkage.

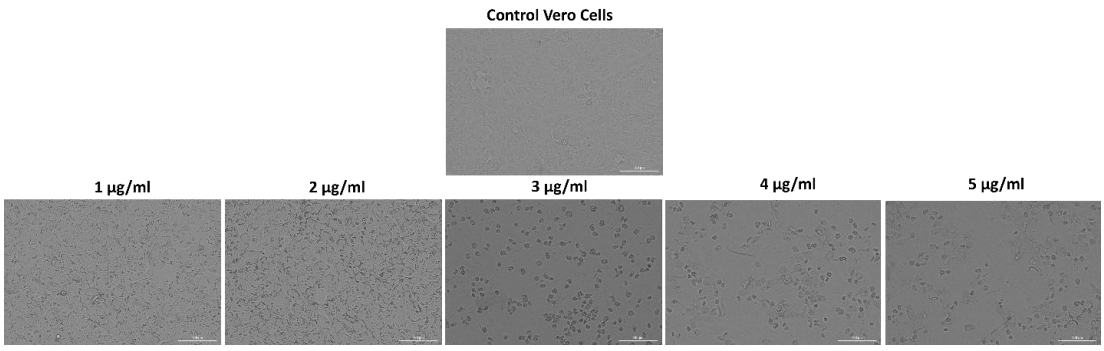

Figure 5.

Representative images of the morphology of Vero cells treated with different concentrations of MCS_OA (1 - 5 µg/mL) for 24 h. Scale bars = 100 µm

Cell morphology is a gold standard, being essential for identifying and analysing dynamic changes that occur under various cellular stress conditions. Cell morphological analysis has been integrated into new methods for biomedical applications, including the identification of cell morphogenesis at different stages of the cell cycle [11].

The final step in assessing the cytotoxic impact of MCS_OA in Vero cells consisted of nuclear and mitochondrial assessments. The cells were treated in this experiment with the lowest, middle and highest concentrations (1, 3 and 5 µg/mL, respectively). As shown in Figure 6, in normal Vero cells, a 1 µg/mL concentration of MCS_OA caused slight nuclear and mitochondrial alterations, including decreased confluence and, in some cases, nuclear condensation. A concentration of 3 µg/mL caused cell nuclei to shrink and condense, and mitochondria appeared slightly condensed in places.

At the highest concentration (5 µg/mL), the most significant reduction in confluence was observed, with significantly shrunken and condensed nuclei compared to the control, and mitochondria also appeared condensed.

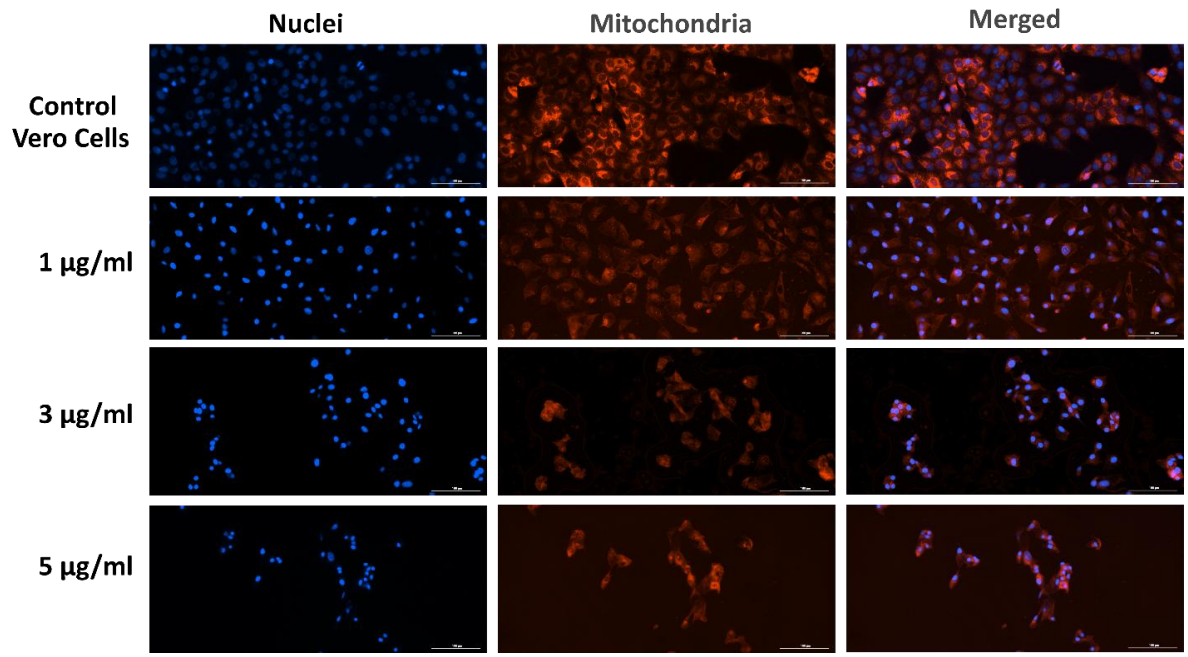

Figure 6.
Representative images of the morphology of nuclei and mitochondria of Vero cells treated with MCS_OA only at 1, 3 and 5 µg/mL concentration for 24 hours. Scale bars = 100 µm

Dysmorphologies occurring in nuclear organisation can affect cellular activities. The nucleus represents a regulatory centre within cells that controls multiple aspects of cellular functions [82]. The technique used in this paper to evaluate nuclei, namely Hoechst, is extensively used in biological, pathological and molecular research, as it is cost-effective and non-toxic [36]. Magnetic fluids are agents of interest, even in oncology. These fluids have multiple applications, including targeted drug delivery, diagnosis and therapy [6].
Considering all this, future biological studies should expand the dose range to identify an optimal concentration that does not significantly affect cells, with dose optimisation as a priority in upcoming research. The sample of interest can also be tested in other experimental models, in 3D-reconstructed tissues and *in ovo* to assess its irritant potential. In addition, *in vivo* investigations could provide further information to help translate the findings into clinical practice. All these assessments are a priority before testing antitumour activity.

Conclusions

The synthesised magnetic colloidal suspension (MCS_OA) based on magnetic iron oxide nanoparticles (MIONPs), double-coated with oleic acid (OA) and dispersed in aqueous solution, exhibits suitable physico-chemical properties, making this a promising candidate for further *in vitro* biomedical evaluation, especially on renal cells.

The *in vitro* biological assessments demonstrated that the MCS_OA sample exhibits a dose-dependent cytotoxic effect on Vero renal cells, with higher concentrations resulting in a significant decrease in cell viability after 24 hours. The results of bright-field morphological analysis and nuclear and mitochondrial analyses of renal cells were consistent with the cell viability results, confirming a concentration-dependent decrease after 24 hours of treatment.
Overall, our preliminary conclusions regarding the toxicity profile support further research on the formulation obtained, including for the treatment of renal cancer, although further in-depth investigations are needed, including the establishment of a dose window that avoids damage to healthy tissues or cells (given that exposure of renal cells to ≥ 3 µg/mL leads to pronounced cytotoxicity), as well as assessments of the mechanisms involved and *in vivo* studies, before clinical translation.

Conflict of interest

The authors declare no conflict of interest.

References

1. Anton N, Bally F, Serra CA, Ali A, Arntz Y, Mely Y, Zhao M, Marchioni E, Jakhmolaa A, Vandamme TF, A new microfluidic setup for precise control of the polymer nanoprecipitation process and lipophilic drug encapsulation. *Soft Matter.*, 2012; 8: 10628-10635.
2. ATCC, www.lgcstandards.com/GB/en/ATCC/cat/362006?utm_campaign=LGC_(Brand)_(ATCC)_R

OE_English&utm_medium=cpc&utm_source=bing&msclkid=0b30d7c47c901dd58b95bed95ea26499.
3. Basak D, Arrighi S, Darwiche Y, Deb S, Comparison of anticancer drug toxicities: paradigm shift in adverse effect profile. *Life (Basel)*, 2021; 12(1): 48-71.
4. Betancur-Granados N, Restrepo JC, Tobón JI, Restrepo-Baena OJ, Dicalcium silicate ($2CaO \cdot SiO_2$) synthesized through flame spray pyrolysis and solution combustion synthesis methods. *Ceram Int.*, 2019; 45(7): 9589-9595.
5. Bica D, Vekas L, Avdeev MV, Marinica O, Socoliuc V, Balasoiu M, Garamus VM, Sterically stabilised water based magnetic fluids: synthesis, structure, and properties. *J Magn Magn Mater*., 2007; 311: 17-21.
6. Bhardwaj A, Jain N, Parekh K, Investigating the effect of outer layer of magnetic particles on cervical cancer cells HeLa by magnetic fluid hyperthermia. *Cancer Nano.*, 2021; 12(7): 1-19.
7. Boyer C, Whittaker MR, Bulmus V, Liu J, Davis TP, The design and utility of polymer stabilised iron oxide nanoparticles for nanomedicine applications. *NPG Asia Mater.*, 2010; 2: 23-30.
8. Buzea C, Pacheco Blandino II, Robbie K, Nanomaterials and nanoparticles: sources and toxicity. *Biointerphases*, 2007; 2: MR17-MR172.
9. Cardoso VF, Francesko A, Ribeiro C, Bañobre-López M, Martins P, Lanceros-Mendez S, Advances in Magnetic Nanoparticles for Biomedical Applications. *Adv Healthc Mater*., 2018; 7(5): 1700845-1700880.
10. Chan MH, Huang WT, Wang J, Liu RS, Hsiao M, Next-Generation Cancer-Specific Hybrid Theranostic Nanomaterials: MAGE-A3 NIR Persistent Luminescence Nanoparticles Conjugated to Afatinib for *In Situ* Suppression of Lung Adenocarcinoma Growth and Metastasis. *Adv Sci (Weinh)*., 2020; 7(9): 1903741-1903756.
11. Chen S, Zhao M, Wu G, Yao C, Zhang J, Recent advances in morphological cell image analysis. *Comput Math Methods Med*., 2012; 2012: 101536-101546.
12. Chen T, Mori Y, Inui-Yamamoto C, Komai Y, Tago Y, Yoshida S, Takabatake Y, Isaka Y, Ohno K, Yoshioka Y, Polymer-brush-afforded SPIO Nanoparticles Show a Unique Biodistribution and MR Imaging Contrast in Mouse Organs. *Magn Reson Med Sci.*, 2017; 16(4): 275-283.
13. Chen X, Wu D, Chen Z, Biomedical applications of stimuli-responsive nanomaterials. *MedComm.*, 2024; 5(8): e643-e679.
14. Chen Z, Liu M, Natural Compounds in Cancer Therapy: Revealing the Role of Flavonoids in Renal Cell Carcinoma Treatment. *Biomolecules*, 2025; 15(5): 620-642.
15. Cirillo L, Innocenti S, Becherucci F, Global epidemiology of kidney cancer. *Nephrol Dial Transplant.*, 2024; 39(6): 920-928.
16. Coricovac DE, Moacă EA, Pinzaru I, Cîtu C, Soica C, Mihali CV, Păcurariu C, Tutelyan VA, Tsatsakis A, Dehelean CA, Biocompatible Colloidal Suspensions Based on Magnetic Iron Oxide Nanoparticles: Synthesis, Characterization and Toxicological Profile. *Front Pharmacol*., 2017; 8: 154-172.
17. Daldrup-Link HE, Rudelius M, Piontek G, Metz S, Bräuer R, Debus G, Corot C, Schlegel J, Link TM, Peschel C, Rummeny EJ, Oostendorp RA, Migration of iron oxide-labeled human hematopoietic progenitor cells in a mouse model: *in vivo* monitoring with 1.5-T MR imaging equipment. *Radiology*, 2005; 234(1): 197-205.
18. Danhier P, De Preter G, Magat J, Godechal Q, Porporato PE, Jordan BF, Feron O, Sonveaux P, Gallez B, Multimodal cell tracking of a spontaneous metastasis model: comparison between MRI, electron paramagnetic resonance and bioluminescence. *Contrast Media Mol Imaging*, 2014; 9(2): 143-153.
19. Danhier P, Magat J, Levêque P, De Preter G, Porporato PE, Bouzin C, Jordan BF, Demeur G, Haufroid V, Feron O, Sonveaux P, Gallez B, *In vivo* visualization and *ex vivo* quantification of murine breast cancer cells in the mouse brain using MRI cell tracking and electron paramagnetic resonance. *NMR Biomed.*, 2015; 28(3): 367-375.
20. Darbandi M, Stromberg F, Landers J, Reckers N, Sanyal B, Keune W, Wende H, Nanoscale size effect on surface spin canting in iron oxide nanoparticles synthesized by the microemulsion method. *J Phys D 45.*, 2012; 45(19): 195001-195012.
21. Das R, Cardarelli JA, Phan MH, Srikanth H, Magnetically tunable iron oxide nanotubes for multifunctional biomedical applications. *J Alloys Compd*., 2019; 789: 323-329.
22. Dulińska-Litewka J, Łazarczyk A, Hałubiec P, Szafrański O, Karnas K, Karewicz A, Superparamagnetic Iron Oxide Nanoparticles-Current and Prospective Medical Applications. *Materials (Basel)*, 2019; 12(4): 617-643.
23. Dürr S, Janko C, Lyer S, Tripal P, Schwarz M, Zaloga J, Tietze R, Alexiou C, Magnetic nanoparticles for cancer therapy. *Nanotech Rev.*, 2013; 2(4), 395-409.
24. Estelrich J, Escribano E, Queralt J, Busquets MA, Iron oxide nanoparticles for magnetically-guided and magnetically-responsive drug delivery. *Int J Mol Sci.*, 2015; 16: 8070-8101.
25. Farcas CG, Dehelean C, Pinzaru IA, Mioc M, Socoliuc V, Moaca EA, Avram S, Ghiulai R, Coricovac D, Pavel I, Alla PK, Cretu OM, Soica C, Loghin F. Thermosensitive betulinic acid-loaded magnetoliposomes: a promising antitumor potential for highly aggressive human breast adenocarcinoma cells under hyperthermic conditions. *Int J Nanomedicine.*, 2020; 15: 8175-8200.
26. Fuentes-García JA, Diaz-Cano AI, Guillen-Cervantes A, Santoyo-Salazar J, Magnetic domain interactions of Fe_3O_4 nanoparticles embedded in a SiO_2 matrix. *Sci Rep.*, 2018; 8(1): 5096-5106.
27. Gholizadeh A, A comparative study of physical properties in Fe_3O_4 nanoparticles prepared by coprecipitation and citrate methods. *J Am Ceram Soc.*, 2017; 100(8): 3577-3588.
28. Gao G, Liu X, Shi R, Zhou K, Shi Y, Ma R, Takayama-Muromachi F, Qiu G, Shape-Controlled Synthesis and Magnetic Properties of Monodisperse Fe_3O_4 Nanocubes. *Cryst Growth Des.*, 2010; 10(7): 2888-2894.
29. Gupta AK, Gupta M, Synthesis and surface engineering of iron oxide nanoparticles for biomedical applications. *Rev Biomater.*, 2005; 26: 3995-4021.
30. Healy S, Bakuzis AF, Goodwill PW, Attaluri A, Bulte JWM, Ivkov R, Clinical magnetic hyperthermia requires

integrated magnetic particle imaging. *WIREs Nanomed Nanobiotechnol.*, 2022; 14(3): e1779-e1799.
31. Heidari P, Masoudpanah SM, Structural and magnetic properties of $MgFe_2O_4$ powders synthesized by solution combustion method: the effect of fuel type. *J Mater Res Technol.*, 2020; (3): 4469-4475.
32. Hufschmid R, Arami H, Ferguson RM, Gonzales M, Teeman E, Brush LN, Browning ND, Krishnan KM, Synthesis of phase-pure and monodisperse iron oxide nanoparticles by thermal decomposition. *Nanoscale*, 2015; 7: 11142-11154.
33. Ianoş R, Tăculescu A, Păcurariu C, Lazău I, Solution Combustion Synthesis and Characterization of Magnetite, Fe_3O_4, Nanopowders. *J Am Ceram Soc*., 2012; 1-5.
34. Ianos R, Istratie R, Pacurariu C, Lazau R, Solution combustion synthesis of strontium aluminate, $SrAl_2O_4$, powders: single-fuel *versus* fuel-mixture approach. *Phys Chem Chem Phys*., 2016; 18(2): 1150-1157.
35. Ianos R, Babuta R, Pacurariu C, Lazau R, Istratie R, Butaciu C, Combustion synthesis of $ZnAl_2O_4$ powders with tuned surface area. *Ceram Int.*, 2017; 43(12): 8975-8981.
36. Iliescu D, Marcovici I, Susan M, Susan R, Pinzaru I, Dumache R, Chiriac S, *In vitro* evaluation of alpha-tocopherol as potential agent in combating the hepatotoxicity induced by ethinylestradiol. *Farmacia*, 2023; 71(3): 533-540.
37. Ittrich H, Lange C, Tögel F, Zander AR, Dahnke H, Westenfelder C, Adam G, Nolte-Ernsting C, *In vivo* magnetic resonance imaging of iron oxide-labeled, arterially-injected mesenchymal stem cells in kidneys of rats with acute ischemic kidney injury: detection and monitoring at 3T. *J Magn Reson Imaging.*, 2007; 25(6): 1179-1191.
38. Kim EH, Lee HS, Kwak BK, Kim BK, Synthesis of ferrofluid with magnetic nanoparticles by sonochemical method for MRI contrast agent. *J Magn Magn Mater*., 2005; 289: 328-330.
39. Kucharczyk K, Rybka JD, Hilgendorff M, Krupinski M, Slachcinski M, Mackiewicz A, Giersig M, Dams-Kozlowska H, Composite spheres made of bioengineered spider silk and iron oxide nanoparticles for theranostics applications. *PLoS One*, 2019; 14(7): e0219790-e0219810.
40. Kudr J, Haddad Y, Richtera L, Heger Z, Cernak M, Adam V, Zitka O, Magnetic nanoparticles: from design and synthesis to real world applications. *Nanomaterials*, 2017; 7: 243-272.
41. Laurent S, Forge D, Port M, Roch A, Robic C, Elst LV, Muller RN, Magnetic iron oxide nanoparticles: synthesis, stabilization, vectorization, physicochemical characterizations and biological applications. *Chem Rev*., 2008; 108: 2064-2110.
42. Lee SW, Yoon JS, Kang S, Kwon K, Chang KS, Lee SG, Choi SI, Jeong JR, Lee G, Nam KM, Sustainable method for the large scale preparation of Fe_3O_4 nano-crystals. *J Am Ceram Soc.*, 2016; 99(8): 578-584.
43. Li D, Jiang D, Chen M, Xie J, Wu Y, Dang S, Zhang J, An easy fabrication of monodisperse oleic acid-coated Fe_3O_4 nanoparticles. *Mater Lett.*, 2010; 64: 2462-2464.
44. Liu M, Wang L, Lo Y, Shiu SC-C, Kinghorn AB, Tanner JA, Aptamer-Enabled Nanomaterials for Therapeutics, Drug Targeting and Imaging. *Cells*, 2022; 11(1): 159-192.
45. Lopes IMD, de Oliveira IM, Bargi-Souza P, Cavallin MD, Kolc CSM, Khalil NM, Quináia SP, Romano MA, Romano RM, Effects of Silver Nanoparticle Exposure to the Testicular Antioxidant System during the Prepubertal Rat Stage. *Chem Res Toxicol*., 2019; 32(6): 986-994.
46. Lu C, Li J, Xu K, Yang C, Wang J, Han C, Liu X, Fabrication of mAb G250-SPIO molecular magnetic resonance imaging nanoprobe for the specific detection of renal cell carcinoma *in vitro*. *PLoS One*, 2014; 9(7): e101898-e1019015.
47. Luo Z, Du H, Prospect of different types of magnetic nanoparticles in stem cell therapy. *Stem Cell Rev*., 2020; 16(4): 1-9.
48. Madorran E, Ambrož M, Knez J, Sobočan M, An Overview of the Current State of Cell Viability Assessment Methods Using OECD Classification. *I J Molec Sci.*, 2025; 26(1): 220-238.
49. Mahmoudi M, Sant S, Wang B, Laurent S, Sen T, Superparamagnetic iron oxide nanoparticles (SPIONs): development, surface modification and applications in chemotherapy. *Adv Drug Deliv Rev*., 2011; 63: 24-46.
50. Mahmoudi M, Hofmann H, Rothen-Rutishauser B, Petri-Fink A, Assessing the *in vitro* and *in vivo* toxicity of superparamagnetic iron oxide nanoparticles. *Chem Rev*., 2012; 112: 2323-2338.
51. Marino A, Camponovo A, Degl'Innocenti A, Bartolucci M, Tapeinos C, Martinelli C, De Pasquale D, Santoro F, Mollo V, Arai S, Suzuki M, Harada Y, Petretto A, Ciofani G, Multifunctional temozolomide-loaded lipid superparamagnetic nanovectors: dual targeting and disintegration of glioblastoma spheroids by synergic chemotherapy and hyperthermia treatment. *Nanoscale*, 2019; 11(44): 21227-21248.
52. Medeiros SF, Filizzola JOC, Fonseca VFM, Oliveira PFM, Silva TM, Elaissari A, Santos AM, Synthesis and characterization of stable aqueous dispersion of functionalised double-coated iron oxide nanoparticles. *Mater Lett*., 2015; 160: 522-525.
53. Mishra SK, Kumar BS, Khushu S, Tripathi RP, Gangenahalli G, Increased transverse relaxivity in ultrasmall superparamagnetic iron oxide nanoparticles used as MRI contrast agent for biomedical imaging. *Contrast Media Mol Imaging*, 2016; 11(5): 350-361.
54. Moacă EA, Watz CG, Socoliuc V, Racoviceanu R, Păcurariu C, Ianoş R, Cîntă-Pînzaru S, Tudoran LB, Nekvapil F, Iurciuc S, Şoica C, Dehelean CA, Biocompatible Magnetic Colloidal Suspension Used as a Tool for Localised Hyperthermia in Human Breast Adenocarcinoma Cells: Physicochemical Analysis and Complex *In Vitro* Biological Profile. *Nanomaterials (Basel)*, 2021; 11(5): 1189-1217.
55. Moacă E-A, Socoliuc V, Stoian D, Watz C, Flondor D, Păcurariu C, Ianoş R, Rus CI, Barbu-Tudoran L, Semenescu A, Sarău C, Chevereşan A, Dehelean CA, Synthesis and Characterization of Bioactive Magnetic Nanoparticles from the Perspective of Hyperthermia Applications. *Magnetochemistry*, 2022; 8(11): 145-168.
56. Moise G, Geamantan-Sîrbu A, Vlad CS, Vlad D, Dumitrescu C, Sima L, Quercetin enhances the anti-tumor activity of doxorubicin in IMR-32 neuroblastoma cells. *Farmacia*, 2024; 72(4): 785-793.

57. MTT assay and its use in cell viability and proliferation analysis, www.abcam.com/en-us/knowledge-center/cell-biology/mtt-assay.
58. Mukh-Qasem RA, Gedanken A, Sonochemical synthesis of stable hydrosol of Fe_3O_4 nanoparticles. *J Colloid Interface Sci.*, 2005; 284(2): 489-494.
59. Muntean SG, Nistor MA, Ianos R, Pacurariu C, Capraru A, Surdu VA, Combustion synthesis of Fe_3O_4/Ag/C nanocomposite and application for dyes removal from multicomponent systems. *Appl Surf Sci*., 2019; 481: 825-837.
60. Okoli C, Sanchez-Dominguez M, Boutonnet M, Järås S, Civera C, Solans C, Kuttuva GR, Comparison and functionalization study of microemulsion-prepared magnetic iron oxide nanoparticles. *Langmuir*, 2012; 28: 8479-8485.
61. de Oliveira IM, Cavallin MD, Corrêa DEDC, Razera A, Mariano DD, Ferreira F, Romano MA, Marino Romano R, Proteomic Profiles of Thyroid Gland and Gene Expression of the Hypothalamic-Pituitary-Thyroid Axis Are Modulated by Exposure to AgNPs during Prepubertal Rat Stages. *Chem Res Toxicol*., 2020; 33(10): 2605-2622.
62. Ozer D, Ertekin Z, Pekmez K, Oztas NA, Fuel effects on $Li_2CuP_2O_7$ synthesized by solution combustion method for lithium-ion batteries. *Ceram Int.*, 2019; 45(4): 4626-4630.
63. Parveen S, Misra R, Sahoo SK, Nanoparticles: a boon to drug delivery, therapeutics, diagnostics and imaging. *Nanomedicine*, 2012; 8: 147-166.
64. Patil RM, Shete PB, Thorat ND, Otari SV, Barick KC, Prasad A, Ningthoujam RS, Tiwalea BM, Pawar SH, Non-aqueous to aqueous phase transfer of oleic acid coated iron oxide nanoparticles for hyperthermia application. *RSC Adv*., 2014; 4: 4515-4522.
65. Rebodos RL, Vikesland PJ, Effects of oxidation on the magnetization of nanoparticulate magnetite. *Langmuir*, 2010; 26(22): 16745-16753.
66. Reddy LH, Arias JL, Nicolas J, Couvreur P, Magnetic nanoparticles: design and characterization, toxicity and biocompatibility, pharmaceutical and biomedical applications. *Chem Rev*., 2012; 112(11): 5818-5878.
67. Rombnu R, Iftode OA, Boța M, Predescu IA, Jîjie AR, Vlaia L, Iliescu D, Tulcan C, Assessment of the antitumour potential of *Melissa Officinalis* ethanolic extract on A375 melanoma cells: *in vitro* and *in ovo* approaches. *Farmacia*, 2025; 73(3): 737-747.
68. Rosen JE, Chan L, Shieh DB, Gu FX, Iron oxide nanoparticles for targeted cancer imaging and diagnostics. *Nanomedicine*, 2012; 8(3): 275-290.
69. Saladino GM, Kakadiya R, Ansari SR, Teleki A, Toprak MS, Magnetoresponsive fluorescent core-shell nanoclusters for biomedical applications. *Nanoscale Adv*., 2023; 5(5): 1323-1330.
70. Scelo G, Larose TL, Epidemiology and Risk Factors for Kidney Cancer. *J Clin Oncol*., 2018; 36(36): 3574-3581.
71. Scherer F, Anton M, Schillinger U, Henke J, Bergemann C, Kruger A, Gansbacher B, Plank C, Magnetofection: enhancing and targeting gene delivery by magnetic force *in vitro* and *in vivo*. *Gene Ther.*, 2002; 9: 102-109.
72. Schneider MGM, Lassalle VL, Magnetic iron oxide nanoparticles as novel and efficient tools for atherosclerosis diagnosis. *Biomed Pharmacother*., 2017; 93: 1098-1115.
73. Senkuttuvan N, Komarasamy B, Krishnamoorthy R, Sarkar S, Dhanasekarand S, Anaikutti P, The significance of chirality in contemporary drug discovery - a mini review. *RSC Adv.*, 2024, 14: 33429-33448.
74. Sharma S, Choudhary N, Verma MK, Sharma ND, Singh D, Cation distribution and magnetic properties of nano and bulk $CoCrFeO_4$ ferrite synthesized by glycinenitrate combustion method. *Ceram Int.*, 2017; 43(14): 11083-11089.
75. Shen Z, Wu A, Chen X, Iron Oxide Nanoparticle-Based Contrast Agents for Magnetic Resonance Imaging. *Mol Pharm*., 2017; 14(5): 1352-1364.
76. Sherikar BN, Sahoo B, Umarji AM, One-step synthesis of diopside ($CaMgSi_2O_6$) ceramic powder by solution combustion method. *Adv Powder Technol*., 2020; 31(8): 3492-3499.
77. Seruga B, Gan HK, Knox JJ, Managing toxicities and optimal dosing of targeted drugs in advanced kidney cancer. *Curr Oncol.*, 2009; 16(Suppl 1): S52-59.
78. Shete PB, Patil RM, Tiwale BM, Pawar SH, Water dispersible oleic acid-coated Fe3O4 nanoparticles for biomedical applications. *J Magn Magn Mater*., 2015; 377: 406-410.
79. Sima L, Tirziu R, Iliescu D, Blidisel A, Hut F, Streian C, Spontaneous rupture of gastroduodenal artery aneurysm. *Chirurgia (Bucur.)*, 2010; 105(5): 717-720.
80. Singh R, Sharma A, Saji J, Umapathi A, Kumar S, Daima HK, Smart nanomaterials for cancer diagnosis and treatment. *Nano Converg*., 2022; 9(1): 21-60.
81. Sirivat A, Paradee N, Facile synthesis of gelatin-coated Fe_3O_4 nanoparticle: effect of pH in single-step co-precipitation for cancer drug loading. *Mater Des*., 2019; 181: 107942-107950.
82. Smeu A, Minda D, Boru C, Vlaia L, Vlaia V, Dehelean CA, Liga S, Puenea G, Muntean DL, Betulinic Acid-Loaded Oleogel as a Novel Pharmaceutical Formulation for Potential Cutaneous Applications: Development, Characterization, and Biosafety Profile. *Life*, 2025; 15(6): 954-977.
83. Soares PI, Lochte F, Echeverria C, Pereira LC, Coutinho JT, Ferreira IM, Novo CM, Borges JP, Thermal and magnetic properties of iron oxide colloids: influence of surfactants. *Nanotechnology*, 2015; 26: 425704-425716.
84. Sun T, Zhang YS, Pang B, Hyun DC, Yang M, Xia Y, Engineered nanoparticles for drug delivery in cancer therapy. *Angew Chem Int Ed Engl*., 2014; 53(46): 12320-12364.
85. Sudheesh VD, Thomas N, Roona N, Baghya PK, Varkey S, Synthesis, characterization and influence of fuel to oxidizer ratio on the properties of spinel ferrite (MFe_2O_4, M = Co and Ni) prepared by solution combustion method. *Ceram Int.*, 2017; 43(17): 15002-15009.
86. Tiwari H, Rai N, Singh S, Gupta P, Verma A, Singh AK, Kajal, Salvi P, Singh SK, Gautam V, Recent advances in nanomaterials-based targeted drug delivery for preclinical cancer diagnosis and therapeutics. *Bioengineering (Basel)*, 2023; 10(7): 760-790.
87. Tomaszewski JJ, Uzzo RG, Kutikov A, Hrebinko K, Mehrazin R, Corcoran A, Ginzburg S, Viterbo R,

Chen DY, Greenberg RE, Smaldone MC, Assessing the burden of complications after surgery for clinically localised kidney cancer by age and comorbidity status. *Urology*, 2014; 83(4): 843-849.

88. Tran HV, Ngo NM, Medhi R, Srinoi P, Liu T, Rittikulsittichai S, Lee TR, Multifunctional Iron Oxide Magnetic Nanoparticles for Biomedical Applications: A Review. *Materials*, 2022; 15(2): 503-550.
89. U.S. Department of Health and Human Services National Institutes of Health National Cancer Institute USA.gov. 2025, www.cancer.gov/types/kidney/patient/kidney-treatment-pdq.
90. Wu W, Wu Z, Yu T, Jiang C, Kim WS, Recent progress on magnetic iron oxide nanoparticles: synthesis, surface functional strategies and biomedical applications. *Sci Technol Adv Mater.*, 2015; 16: 023501-023544.
91. Wu W, Jiang CZ, Roy VA, Designed synthesis and surface engineering strategies of magnetic iron oxide nanoparticles for biomedical applications. *Nanoscale*, 2016; 8(47): 19421-19474.
92. Xie S, Zhang B, Wang L, Wang J, Li X, Yang G, Superparamagnetic iron oxide nanoparticles coated with different polymers and their MRI contrast effects in the mouse brains. *Appl Surf Sci*., 2015; 326: 32-38.
93. Xie W, Guo Z, Gao F, Gao Q, Wang D, Liaw BS, Cai Q, Sun X, Wang X, Zhao L, Shape-, size- and structure-controlled synthesis and biocompatibility of iron oxide nanoparticles for magnetic theranostics. *Theranostics*, 2018; 8(12): 3284-3307.
94. Zhang L, He R, Gu HC, Oleic acid coating on the monodisperse magnetite nanoparticles. *Appl Surf Sci*., 2006; 253: 2611-2617.
95. Zhang Y, Jia Y, A facile precursor calcination approach to iron oxide micro/nanostructures with a high magnetization. *J Alloys Compd*., 2016; 659: 66-73.